

The Behavior of an Isolated Free Eddy in a Rotating Fluid (A Laboratory Experiment)

Takematsu, Masaki

Research Institute for Applied Mechanics, Kyushu University : Professor

Kita, Tsugio

Research Institute for Applied Mechanics, Kyushu University : Research Assistant

<https://doi.org/10.5109/6781023>

出版情報 : Reports of Research Institute for Applied Mechanics. 33 (100), pp.1-12, 1985-09. 九州大学応用力学研究所

バージョン :

権利関係 :



The Behavior of an Isolated Free Eddy in a Rotating Fluid (A Laboratory Experiment)

By Masaki TAKEMATSU* and Tsugio KITA**

An isolated cyclonic free eddy was generated in a rotating basin with the (topographic) beta-effect by locally cooling the water surface, and its structure and evolution were observed by means of flow visualization methods.

After an initial adjustment period, the cold core eddy exhibited a fairly good vertical coherence. Clearly the eddy was of the Rankine type having a net circulation ($\Gamma \neq 0$) in contrast to the Gaussian eddy ($\Gamma = 0$). The cyclonic main eddy moved west or southwest (the southward movement took place mainly in the initial adjustment period). Weak vortices and streamings were certainly induced around the main eddy, but the induced flow pattern was of transient nature and quite dissimilar to the "herringbone" pattern predicted by previous numerical experiments for the Gaussian eddy. It is now obvious that the Gaussian eddy cannot necessarily be representative of cyclonic eddies.

Key words: Isolated eddy, Flow visualization

1. Introduction

This note presents some results of a visual study of an isolated free eddy on a (topographic) beta-plane. Probably this is the first laboratory experiment on the subject aside from the earlier attempt of Firing and Beardsley¹⁾ for which a new interpretation will be posed below.

During the past decade considerable numerical effort has been given to the planetary eddy motion, starting with the work of Bretherton and Karweit²⁾. A main conclusion from those numerical simulations is that a nonlinear cyclonic (anticyclonic) eddy moves toward west-northwest (west-southwest) leaving behind a Rossby wave wake with a characteristic herringbone pattern. The present experiment was motivated by the desire to see whether a cyclonic eddy really behaves as described above. However, it should be reminded that initial eddies considered in the existing numerical simulations are all of the

* Professor, Research Institute for Applied Mechanics, Kyushu University, Kasuga 816, Japan

** Research Assistant, Research Institute for Applied Mechanics.

Gaussian type. By contrast, cyclonic eddies generated in our experiment are naturally of the well-know Rankine type. A distinctive feature of Gaussian eddies is that they have the zero net circulation ($\Gamma=0$) and hence are essentially "inert" (namely, on an f -plane they cannot interact with other eddies except by direct collision). There seems to be no *a priori* reason to expect that the two types of cyclonic eddies exhibit the same behavior.

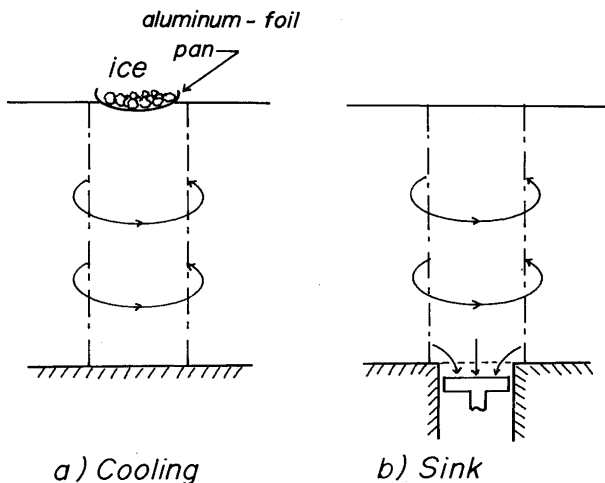


Fig.1 Methods of generating an isolated free eddy in a rotating system.

In a rotating system, a cyclonic eddy of the Rankine type can be easily generated by local cooling of the water surface (Fig.1,a) or by a sink distribution at the basin bottom (Fig.1,b); similarly an appropriate divergent flow can induce an anticyclonic eddy. In this experiment the former (cooling) method was adopted for generating free cyclonic eddies.

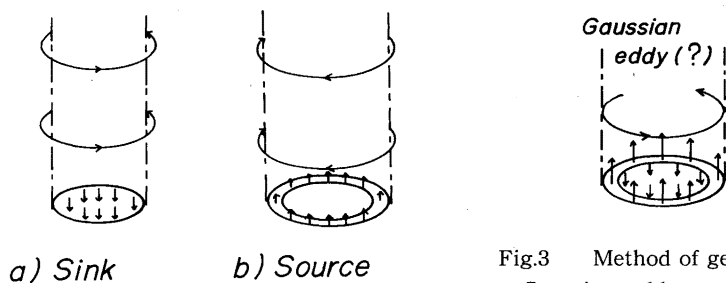


Fig.2 Circular distributions of sink and source.

Fig.3 Method of generating a Gaussian eddy employed by Firing and Beardsley.

For the purpose of comparison with numerical results, it would be more convenient to work with a Gaussian eddy. The task was once attempted by Firing and Beardsley¹⁾. Now consider a circular sink and source of equal strength as depicted in Fig.2, which are respectively capable of generating a cyclonic and

an anticyclonic eddy of the Rankine type. One might suppose, as Firing and Beardsley did, that a concentric combination of the two forcings (Fig.3) could successfully give rise to a single cyclonic Gaussian eddy. However, it must be borne in mind that the formation of a quasi-geostrophic eddy motion is necessarily preceded by rather complicated adjustment processes starting with a three-dimensional potential flow (somehow Firing and Beardsley ignored this important fact). The designed symmetry of the forcing is unlikely to survive the adjustment period, in particular, in the presence of a topographic asymmetry (i. e., on a beta-plane); most likely the concentric forcing will result in a pair of eddies. Then it may be reasonable to suspect that Firing and Beardsley must have unintentionally worked with a pair of eddies instead of a single Gaussian eddy. Indeed, the photos of their Fig.3 clearly show the appearance of an eddy pair, but nothing else. The two dominant eddies (seemingly of equal strength) may be respectively due to the inner piston (sink) and the outer one (source) of their generating device, and have nothing to do with their computations for a Gaussian eddy. This is a new interpretation for the widely quoted experiment of Firing and Beardsley.

2. Experimental aspects

The apparatus used in this experiment is schematically shown in Fig.4. Major parameters of the apparatus and other relevant informations are as follows:

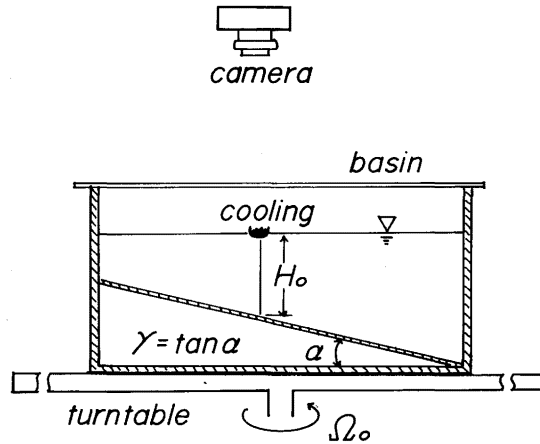


Fig.4 Schematic diagram of the experimental apparatus.

- The angular velocity (Ω_0) of the turntable (200 cm diameter) is $2\pi/15 \sim 2\pi/18$ rad/sec in the counter-clockwise direction.
- Use is made of four different basins; i.e., two circular basins (80 cm-, 40 cm diameter) and two square ones (40cm \times 40cm, 20cm \times 18cm). The water depth (H_0) as measured at the center of each eddy is 4cm \sim 8cm.
- The bottom slope γ ($=\tan\alpha$) is 1/3, 1/4 and 1/6. The beta-parameter

defined by $\beta = 2\Omega_0\gamma/H_0$ is then $0.015 \sim 0.070$ rad/cm sec.

d) Local cooling is done by an aluminum-foil pan loaded with a small amount (typically 0.5g) of ice flake. Direct cooling by an ice cube (about 1.5cm) is also attempted.

e) Flow visualization is carried out by means of the aluminum powder method and the thymol blue method. Fine vertical lines made by sinking methylene blue powder are also useful for the purpose of observing the vertical structure of eddies.

f) A representative eddy radius (ℓ) appears to be $1\text{cm} \sim 3\text{cm}$ (of the same order of the inner deformation radius). A typical rotation velocity (U) of the eddy motion is initially about 1cm/sec and then decreases to zero as time goes on.

The characteristics of the eddy motion may be summarized as

$$\begin{cases} f = 2\Omega_0 & \cdots \cdots 0.70 \sim 0.85 \text{ rad/sec} \\ \beta \ell & \cdots \cdots 0.02 \sim 0.20 \\ U/\ell & \cdots \cdots < 1 \quad / \text{sec}, \end{cases}$$

where the first is the Coriolis parameter, the second the variation of the Coriolis parameter and the third a measure of the relative vorticity of the eddy motion.

3. Experimental results

After a number of preliminary visual observations under a wide variety of experimental conditions, photographic records of typical flow patterns were taken at appropriate fixed intervals. Some selected results of interest will be presented next, where the lapse of time after the onset of forcing (cooling) will be expressed, for convenience, in terms of the basic rotation period $T = 2\pi/\Omega_0$ (15 sec-18 sec).

After an initial adjustment period ($< 3T$), a vertically coherent eddy field was established. The resulting flow field consisted of a central cyclonic eddy (hereafter referred to as a main eddy) and a surrounding field of weak but wide-spread streaming. Fig.5 is a typical flow pattern of the main eddy visualized by methylene blue powder spread over the water surface. The main eddy was very stable and retained a nearly circular pattern throughout its lifetime ($> 40T$). As will be demonstrated below, the main eddy moved toward west or southwest unless affected by side boundaries; when it approached a side wall, it moved parallel to the wall according to the well-known rule of the classical vortex theory. Note that the surrounding weak spiral extended as far as some 20 cm from the center of the eddy. (Hence, an eddy in a relatively small basin would soon feel the influence of boundaries). In contrast to the main eddy, the surrounding field was highly variable.

Fig.6 shows a sequence of aluminum powder photographs of eddy motion, illustrating the behavior of the main eddy and time evolution of surrounding flow patterns. (The photographs were taken at horizontal level 1.5cm below the water surface with a shutter opening of 8 sec. Streamline patterns at lower levels were also photographed and found to be essentially the same as those presented). It may be seen that the main eddy moved toward west (with a mean speed of about 0.05 cm/sec) accompanied with induced eddies and streamings of transient

nature. Such weak transient eddies, which tend to appear to the south of the main eddy, are unlikely to have any appreciable effect upon the behavior of the main eddy. Naturally, the wide-spread weak surrounding field is liable to be affected by the presence of side boundaries. Fig.7 shows a streamline pattern around a main eddy generated in a smaller basin ($20\text{cm} \times 18\text{cm}$), illustrating the influence of the side walls; the induced flow patterns around the main eddy were different from those in a larger basin (see, for example, Fig.6 b)), but the behavior of the main eddy was little affected until it approached a wall excessively. (For the purpose of evaluating the effect of side boundaries, Mied and Lindemann³⁾ examined changes in the central pressure of main eddies. However, it should be kept in mind that the strength of a main eddy is the least sensitive indicator for the purpose).

The eddy motion as visualized by the thymol blue method is shown in Fig. 8, where the dye release was started before the onset of cooling and continued during the course of observation. Those photographs illustrate the transient and complicated nature of the surrounding field (lighter and diffused dye lines are lingering traces of earlier flow patterns). The part of dye lines within the main eddy was blown off due to excessive flow velocities. It may be seen from the sequence of photographs that this main eddy moved toward southwest.

During the initial cooling period, a cold core eddy is gradually formed as it moves toward south (down slope) together with the cooling device (a cooling pan or an ice cube). Then, if the cooling is done with the cooling device fixed, a variety of complicated flow patterns appear. An example is shown in Fig.9. In this case there happened to appear a pair of eddies, a cyclonic eddy and a weaker anticyclonic eddy (photo a)). The cyclonic eddy of elliptic form (a Kirchhoff eddy?) rotated in the cyclonic direction entraining the anticyclonic eddy (photo b)). During the course of the experiment, other various aspects of eddy-eddy and eddy-wall interactions were observed.

4. Concluding remarks

Isolated cyclonic free eddies were generated in rotating basins and observed by means of flow visualization methods. The resulting eddies seem to be ordinary eddies akin to those in the oceans, but their behaviors are found to be different in various essential respects from previous numerical predictions. It appears that previous investigators have erred on the side of numerical simulations for Gaussian eddies. Hopefully, the present experiment may serve as a new step for developing a sound theory on the subject.

Finally we note that anyone can repeat the same experiment without any difficulty only if a simple turntable and a small amount of ice are available.

Acknowledgments

The authors wish to thank Dr. A. Masuda and Prof. H. Honji for their critical discussion and interest in this work.

Reference

- 1) Firing, E., and R.C. Beardsley : J. Phys. Oceanogr., 6 (1976) 57-65.
- 2) Bretherton, F.P., and M. Karweit : *Numerical Models of Ocean Circulation Proceedings* (National Academy of Sciences, 1975) 237-249.
- 3) Mied, R.P., and G.J. Lindemann : J. Phys. Oceanogr., 9 (1979) 1183-1206.

(Received August 20, 1985)

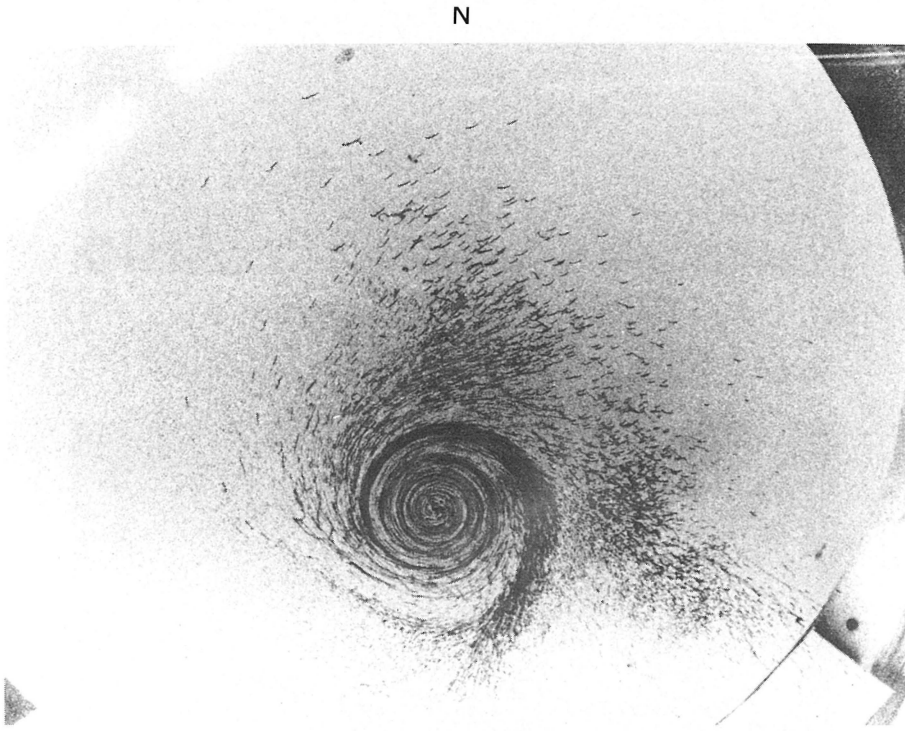


Fig.5 Eddy generated by an ice cube in a circular basin (40cm dia.) : $H_0 = 8$ cm, $\gamma = 1/4$.

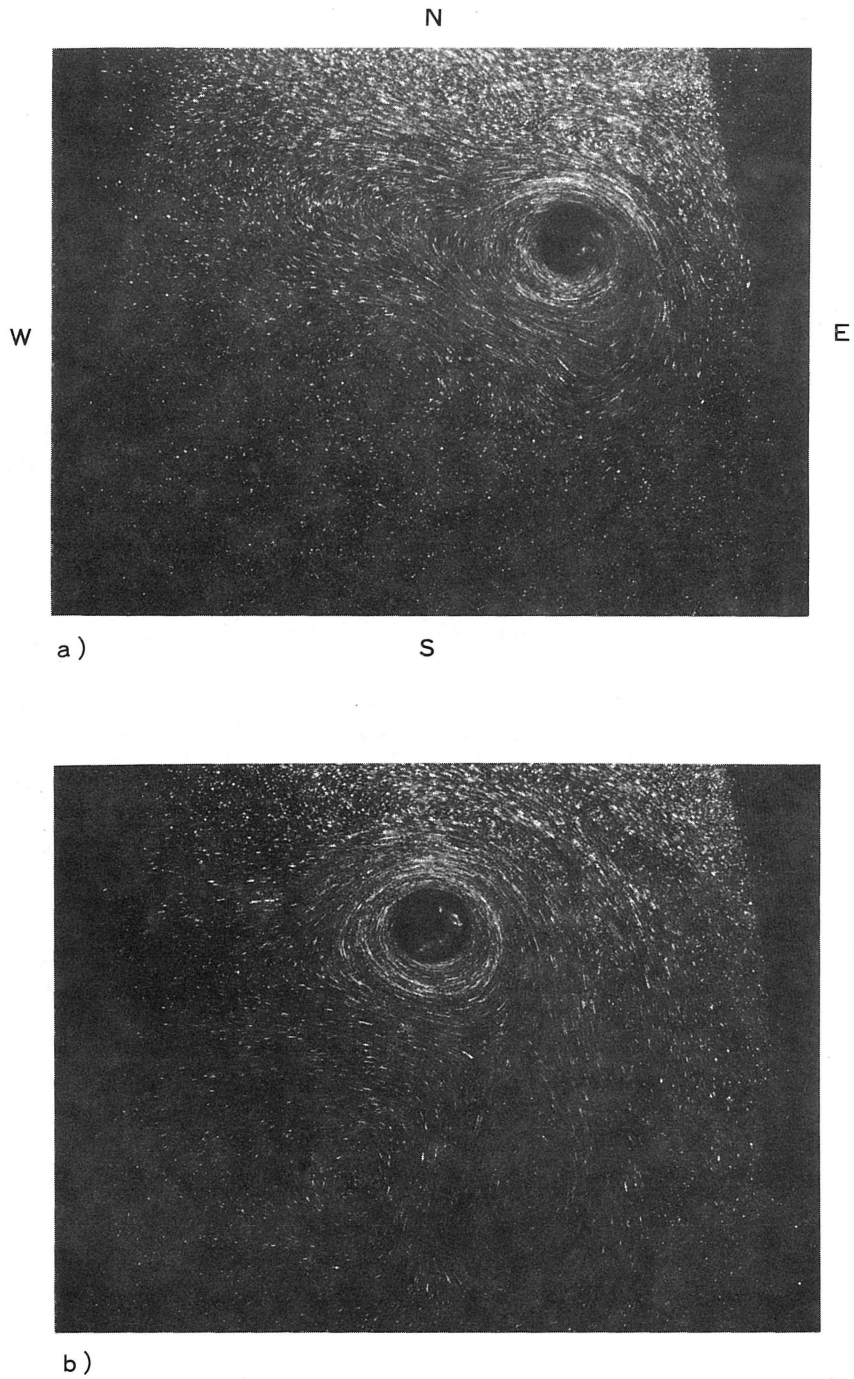
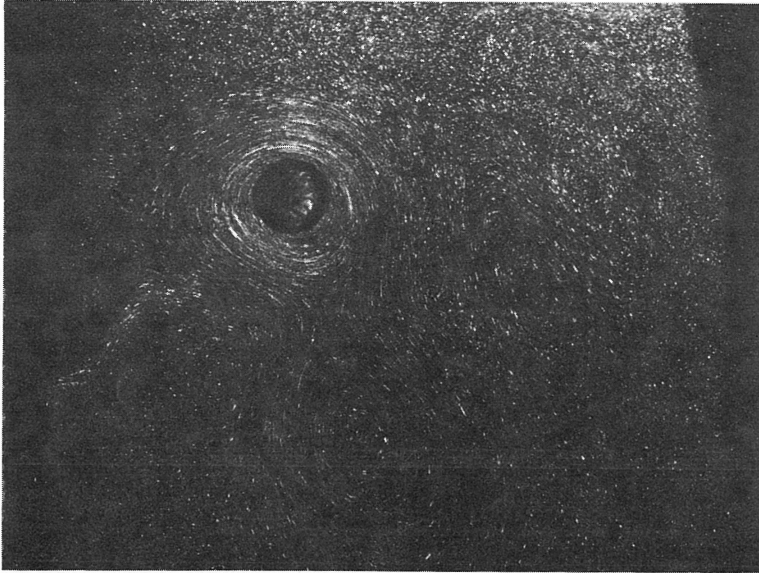
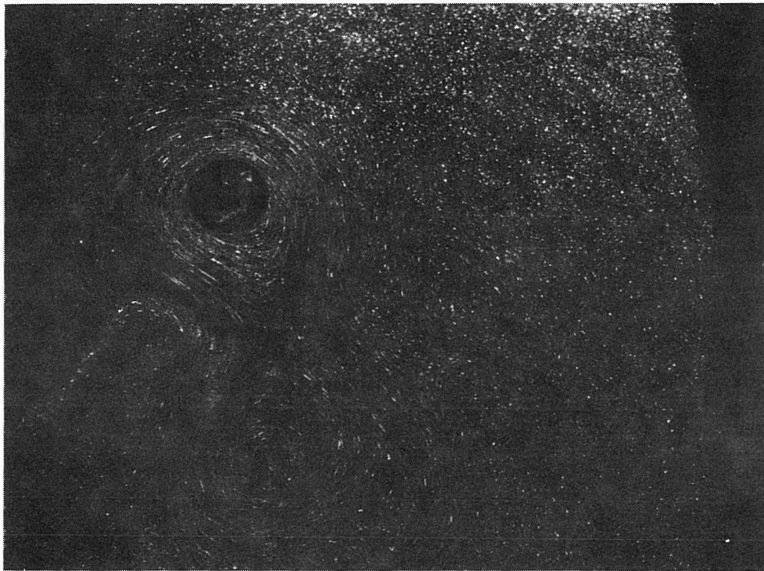


Fig.6 Aluminum powder photographs of an eddy in a square basin ($40\text{cm} \times 40\text{cm}$),
 a) $t=5T$, b) $t=15T$, c) $t=25T$, d) $t=31T$: $H_0=7\text{cm}$, $\gamma=1/4$, $T=17\text{ sec}$.



c)



d)

Fig.6

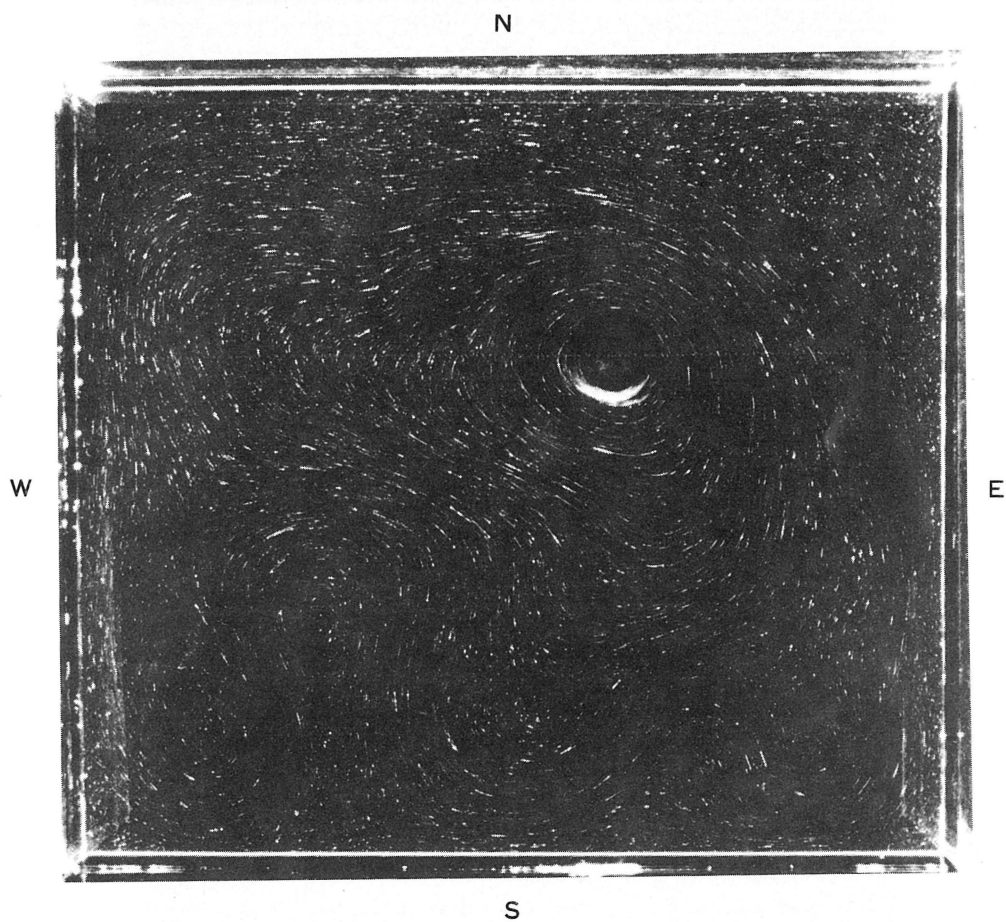
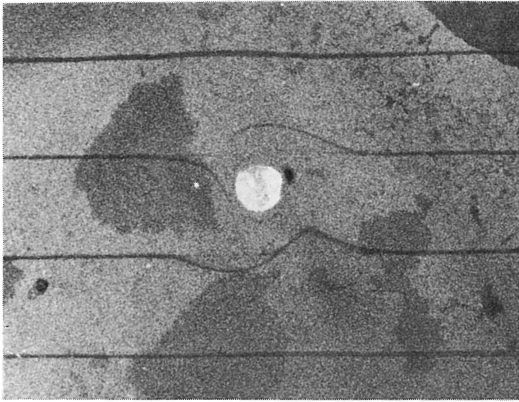
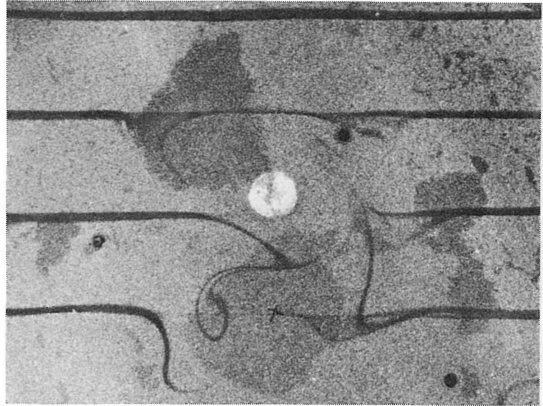


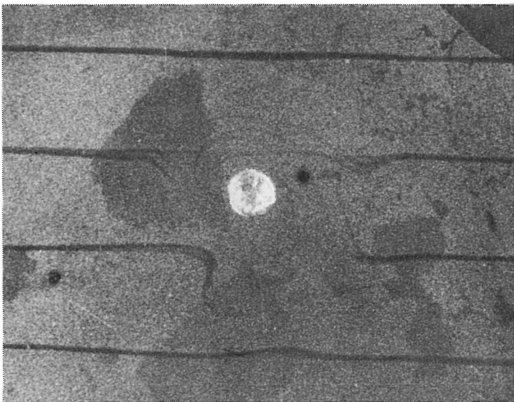
Fig.7 Streamline pattern of an eddy in a smaller basin ($20\text{cm} \times 18\text{cm}$) at $t=10 T$:
 $H_0 = 5\text{cm}$, $\gamma = 1/3$, $T = 17\text{sec}$.



a)



c)



b)

Fig.8 Dye line photographs of an eddy in a circular basin (80cm dia.) , a) $t = 5 T$,
b) $t = 11 T$, c) $t = 21 T$: $H_0 = 8 \text{ cm}$,
 $\gamma = 1/4$, $T = 17.5 \text{ sec}$.



Fig.9 Flow patterns generated by a fixed ice cube, a) $t = 11 T$, b) $t = 19 T$: $H_0 = 8\text{cm}$, $\gamma = 1/4$, $T = 17\text{ sec.}$